THE JOURNAL OF PHYSICAL CHEMISTRY B

Article

pubs.acs.org/JPCB

Phase Behavior of a Lattice Hydrophobic Oligomer in Explicit Water

Santiago Romero-Vargas Castrillón,*[,†,⊥] Silvina Matysiak,[‡] Frank H. Stillinger,[◇] Peter J. Rossky,[§] and Pablo G. Debenedetti[†]

[†]Department of Chemical and Biological Engineering, Princeton University, Princeton, New Jersey 08544, United States

[‡]Fischell Department of Bioengineering, University of Maryland, College Park, Maryland 20742, United States

[◇]Department of Chemistry, Princeton University, Princeton, New Jersey 08544, United States

[§]Institute for Computational Engineering & Sciences and Department of Chemistry and Biochemistry, University of Texas at Austin, Austin, Texas 78712, United States

Supporting Information

ABSTRACT: We investigate the thermodynamics of hydrophobic oligomer collapse using a water-explicit, three-dimensional lattice model. The model captures several aspects of protein thermodynamics, including the emergence of cold- and thermal-unfolding, as well as unfolding at high solvent density (a phenomenon akin to pressure-induced denaturation). We show that over a range of conditions spanning a ≈14% increase in solvent density, the oligomer transforms into a compact, strongly water-penetrated conformation at low temperature. This contrasts with thermal unfolding at high temperature, where the system "denatures" into an extended random coil conformation. We report a phase diagram for hydrophobic collapse that correctly captures qualitative aspects of cold and thermal unfolding at low to intermediate solvent densities.

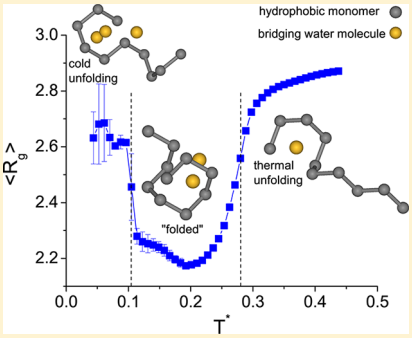

1. INTRODUCTION

Many self-assembly processes in aqueous solution, from the formation of vesicles and micelles to protein folding, are driven by the aversion of hydrophobic moieties for water, the so-called hydrophobic effect. The importance of the hydrophobic effect in biological self-assembly processes was first proposed in 1959 by Kauzmann,[1] who conjectured that hydrophobic interactions, the tendency of hydrophobic moieties to aggregate in water, are the primary driving force behind the folding of a native polypeptide into a biologically active protein. This conjecture is now regarded as a well-accepted fact based on a number of observations. First, hydrophobic amino acids are found at the core of the native structure, where they avoid contact with water, and water-soluble proteins do not fold to active structures in apolar solvents. More importantly, the solution thermodynamics of small hydrocarbons in water exhibits many similarities with the thermodynamics of protein unfolding.[2−4] In both instances, there is a large positive increase in the heat capacity upon hydrocarbon dissolution (or protein unfolding), signaling that both ΔH and $T\Delta S$ increase with temperature. This in turn implies that the T-dependence of the unfolding free energy (ΔG_u) is parabolic, decreasing to negative values at both high and low temperatures.

Proteins exist in their native, biologically active state only within a limited temperature range that is described closely by the T-dependence of the free energy of unfolding. Close to room temperature and ambient pressure, ΔG_u for proteins traverses a maximum and the native state is marginally stable (ΔG_u per residue is less than $1/10k_BT$).[3] Under these conditions, the driving force for folding is entropy-dominated, generally accepted to be brought about by the formation of a more ordered hydration layer around hydrophobic moieties, within which water exhibits a lower hydrogen bond entropy and enthalpy.[5−7,9] By folding the polypeptide into a compact structure with reduced solvent contact, the entropy of the system is maximized. At high temperatures, the native state is destabilized with respect to the unfolded state through the large entropy increase in the unraveled amino acid chain. A similar phenomenon, cold unfolding,[8] has been observed at low temperatures, where the impact of solvent entropy loss is reduced, and the unfolded state is stabilized by enthalpy. Cold unfolding is akin to the low-temperature solubility of hydrophobic solutes.[8]

The "liquid hydrocarbon" model[1] described above successfully describes the T-dependence of protein unfolding but fails to rationalize the pressure (p) dependence. The volume change of thermal unfolding is positive at low p and negative at high p; on the other hand, the volume change upon hydrocarbon dissolution in water exhibits exactly the opposite behavior: negative at low p and positive at high p.[10−12] Hummer et al.,[11] using computer simulations, have rationalized the observed pressure dependence by invoking an inverted liquid hydrocarbon model (conceptualized as the transfer of water to a pure

Received: April 23, 2012
Revised: June 19, 2012
Published: July 23, 2012

   dx.doi.org/10.1021/jp3039237 | J. Phys. Chem. B 2012, 116, 9540−9548

hydrocarbon phase), with protein folds destabilized by pressure because of water penetration of the hydrophobic core.[12]

Molecular simulation studies have revealed considerable insight into the mechanisms by which a protein becomes unfolded or denatured. In particular, atomistic molecular dynamics (MD) simulations have provided microscopic information about, e.g., the role of hydrophobic interactions in the formation of the protein hydrophobic core[13] and the collapse of multidomain proteins,[14] the formation of secondary-structural features such as α-helices and β-hairpins,[15−18] the role of water in pressure-induced denaturation,[19] and the mechanisms of protein unfolding due to denaturants such as urea.[51] Despite the ever-increasing computational power, however, the long time scales characterizing protein dynamics impose limits on the scope of fully atomistic simulations.

An alternative approach[20−25] espouses minimalist models where the protein structure and dynamics are constrained to a lattice, significantly reducing the degrees of freedom relative to continuum MD simulations at the expense of detail. Lattice models such as the HP model[20] have revealed that sequences folding into a unique native conformation can emerge from a simple two-letter, hydrophobic/hydrophilic, amino acid alphabet. Nevertheless, implicit solvent models without temperature-dependent effective interactions cannot capture effects such as cold denaturation.[21] Recently, Patel et al.[26,27] formulated a 2-D lattice model of homo- and heteropolymers in explicit water and carried out simulations using flat-histogram Monte Carlo techniques.[28,29] The authors showed that upon explicit incorporation of the thermodynamics of hydrophobic solvation (namely, the entropic penalty and enthalpic bonus upon interfacial HB formation), the model exhibits cold-, thermal-, and pressure-induced oligomer unfolding.[26] The model was subsequently extended and refined on a 3-D lattice by Matysiak et al.[30] Extension to three dimensions resulted in several improvements, most importantly the ability to correctly capture the hydrogen-bond topology of hydration water. The 3-D lattice model also enables the study of protein secondary structure in a realistic manner. In this respect, the model by Matysiak et al.[30] builds on the pioneering work of Skolnick et al.,[23−25] who proposed a family of lattice models that could produce the secondary-structural aspects of proteins. However, unlike these implicit water models, the work of Matysiak et al.[30] treats water explicitly and is found to exhibit cold- and thermal denaturation.

In this study we use the model of Matysiak et al.[30] to investigate the combined effect of temperature and waterlike solvent density on the conformational stability of a hydrophobic oligomer, a convenient system to study protein thermodynamics.[31] We find that over a range of conditions spanning a 14% increase in water density, the folded oligomer is marginally stable, unfolding at low temperatures into compact, water-penetrated denatured conformations; at hight T, the oligomer unravels into an ensemble of random coils. We find that over the range of densities investigated, the slope of the cold- and thermal-unfolding loci in the $\rho-T$ plane is positive, in agreement with experimentally observed phase behavior.[32] We also study the system at a high water density and find that conformational diversity disappears; we observe a compact, strongly water-penetrated (hence, denatured) oligomer at all temperatures.

This paper is structured as follows: In section 2 we review the lattice model of Matysiak et al.[30] The Wang−Landau flat-histogram technique used to numerically solve the model, as well as the data analysis methodology, are presented in section 3. Results and discussion, followed by a summary and conclusions are presented in sections 4 and 5, respectively.

2. LATTICE MODEL

We study a system at infinite dilution, consisting of a single hydrophobic oligomer in explicit water. The main goal of our work is to study the conformational states of solvated oligomers. Since transitions are strongly cooperative and involve the concerted motion of a large number of water molecules and oligomer residues, the time required to sample these is fairly long. As in numerous previous studies,[20−25] we choose a lattice representation of the system, which reduces the degrees of freedom by constraining molecular positions to the lattice geometry. This coarse-graining significantly reduces the computational resources required to analyze the problem. Previous studies using lattice models have yielded many insights into protein thermodynamics. We should emphasize, however, that, apart from a handful of examples,[21,22] most investigations included water only implicitly. Our study distinguishes itself in that water is represented explicitly on the lattice.

The protein−water system is projected onto a body-centered cubic lattice, which can be alternatively conceptualized as two interpenetrating tetrahedral lattices. Each site possesses eight nearest neighbors (nn), placed at a distance $3^{1/2}$ on the vertices of the cube, so that relative coordinate alternatives $[\pm1, \pm1, \pm1]$ describe virtual bonds between nn lattice sites. Water molecules are described using a modified version of the model by Roberts and Debenedetti,[33,34] which captures many of liquid water's properties, including the density anomaly and the hypothesized existence of two distinct supercooled liquid phases. We have verified that our simulations are conducted under conditions where solvent-phase separation does not affect analysis of oligomer stability (see Supporting Information). The lattice site representing the water oxygen atom is fitted with four bonding arms (two proton donors and two proton acceptors) arranged tetrahedrally. Molecules interact with their nn sites through hydrogen bonding (HB) interactions on the tetrahedral directions. Non-hydrogen-bonded nn sites interact through nondirectional, van der Waals-like interactions. A schematic of the lattice waterlike solvent is shown in Figure 1a. The HB (ε_{HB}) and dispersive (ε_{vdW}) interaction energies depend on the number of nn (N_{nn}) surrounding the interacting pair; this captures the fact that the interaction strength is correlated with N_{nn}.[35−37,53]Interaction parameters were obtained from atomistic molecular dynamics simulations of a polypeptide in water.[37]Further information on the parametrization can be found in the Supporting Information.[30,37]

Molecular orientational degrees of freedom are introduced through a Potts variable $\sigma_i = 1,...,q$, determining the q possible, distinguishable orientations of the molecule occupying site i. Molecules are not restricted to be oriented such that their arms point only toward nn sites. For a HB to be formed, two nn water molecules must have a mutually oriented donor−acceptor pair of bonding arms. Results from MD simulations[6,7] suggest that bulk water molecules frequently sample more distorted HB configurations and, therefore, have a higher orientational entropy. Similarly, MD simulations and spectroscopic studies suggest that water participating in hydrophobic hydration exhibits slower dynamics relative to the bulk liquid[38,40] and a preferential orientation in which HB arms

dx.doi.org/10.1021/jp3039237 | J. Phys. Chem. B 2012, 116, 9540−9548

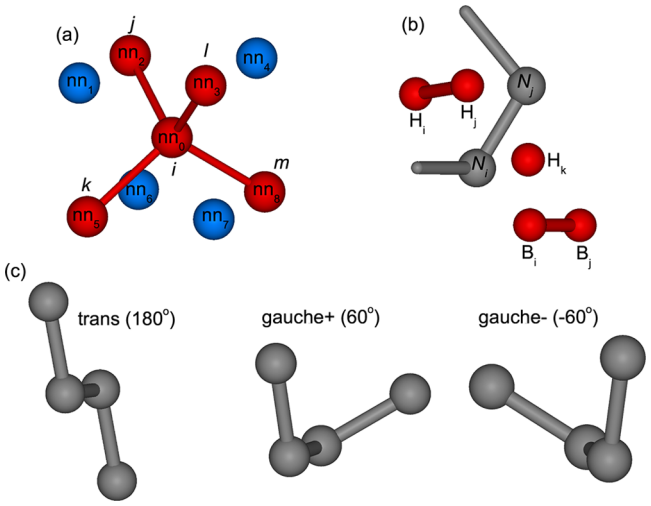

Figure 1. (a) Lattice representation of the waterlike solvent. In the bcc lattice, a central site (labeled nn_0) is surrounded by 8 nearest-neighbor (nn) sites (labeled nn_i; i = 1,...,8). Empty sites are shown as blue spheres, while those occupied by water molecules are shown in red. Hydrogen bonds (HBs), formed by mutually oriented donor−acceptor arms, appear as red lines joining the centers of the hydrogen-bonded molecules. The figure shows molecule i forming four HBs with j, k, l, and m (i.e., the maximum possible number of HBs). The angle between H-bonded entities (e.g., the j−i−k angle) is tetrahedral. The distance between nn sites is $3^{1/2}$. (b) Schematic representation of a solvated oligomer segment comprising two monomers (N_i and N_j, in gray); the surrounding hydration water (H) and bulk water molecules (B) are shown in red. Gray lines denote monomer−monomer covalent bonds between N_i and N_j, and their respective bonded neighbors (not shown). Red lines designate HBs. The entropic penalty of hydrophobic hydration requires that the orientations of H_i and H_j be equal, i.e., $\sigma_{H_i} = \sigma_{H_j}$. H_j and H_k are non-H-bonded nearest neighbors because $\sigma_{H_j} \neq \sigma_{H_k}$; these molecules, therefore, only establish van der Waals-type interactions. For bulk molecules (i.e., non-nn to a monomer), a larger subset of H-bonding orientations is introduced by allowing an orientational mismatch (λ_b), i.e., $|\sigma_{B_i} - \sigma_{B_j}| \leq \lambda_b = 1$. (c) Schematic representation of the different rotational conformations of the oligomer and their respective torsional angles.

are tangential to the solute or residue, allowing water molecules to preserve their HB connectivity.[6,7,37,39] These features of hydrophobic solvation are incorporated into the model following the work of Patel et al.[26] Accordingly, we consider a larger subset of molecular orientations leading to HB formation in the bulk compared to hydration water (i.e., molecules adjacent to one or more monomers), as follows. For pairs of bulk water molecules, a larger range of orientations is introduced by allowing an orientational mismatch, $\lambda_b = 1$. A bulk−bulk HB is thus formed when the orientations of molecules i and j satisfy $|\sigma_i - \sigma_j| \leq \lambda_b$. For hydration-layer water molecules, on the other hand, we require that the orientations match exactly, i.e., $\sigma_i = \sigma_j$. Apart from the entropic penalty, hydration water molecules less frequently sample the more distorted HB configurations observed in the bulk, forming more directional (less-strained) HBs. The stronger HBs formed in the hydration layer are accounted for by an energetic bonus, $\varepsilon_{HB}^{bonus} = -0.2$ kcal/mol, resulting in a HB interaction equal to $\varepsilon''_{HB}(N_{nn}) = \varepsilon_{HB}(N_{nn}) + \varepsilon_{HB}^{bonus}$. For bulk water molecules, the HB interaction energy remains $\varepsilon''_{HB}(N_{nn}) = \varepsilon_{HB}(N_{nn})$. The HB formation criterion is illustrated schematically in Figure 1b. To summarize, water−water interactions are described through the Hamiltonian[30]

$$\mathcal{H}_{w-w} = \frac{1}{2}\sum_{\langle i,j\rangle} nw_i nw_j [\delta_{\sigma_i\sigma_j}\varepsilon''_{HB}(N_{nn}) + (1 - \delta_{\sigma_i\sigma_j})\varepsilon_{vdW}(N_{nn})] \quad (1)$$

In eq 1, the occupation variable nw_i is equal to 1 if site i is occupied by a water molecule, and zero when empty or occupied by a monomer; $\delta_{\sigma_i\sigma_j} = 1$ if the orientations of molecules in nn sites i and j are conducive to hydrogen bonding (i.e., identical orientations if the pair is in the hydration layer, or off by, at most, λ_b if bulk), and zero otherwise. The summation runs over nearest-neighbor pairs.

The oligomer is modeled as a self-avoiding walk in the underlying tetrahedral lattices. Throughout this work we study a hydrophobic oligomer consisting of 10 residues. Our work follows that of Skolnick and collaborators[23−25] as described below. Each point on the lattice occupied by a monomer represents a residue of the hydrophobic oligomer. Monomer−monomer bond lengths are fixed to the aforementioned value of $3^{1/2}$; lattice geometry constrains the angle formed by three consecutive monomers to the tetrahedral value, $\cos^{-1}(-1/3) \approx 109.47°$. The coarse-grained representation allows three distinguishable rotational conformations per every consecutive four monomers: the in-plane trans, characterized by a torsional angle of 180°; the out-of-plane gauche+ and gauche−, characterized by torsional angles of +60° and −60°, respectively.[25,41] We choose to simulate an athermal oligomer in which, aside from forbidding site occupancy by more than 1 monomer, there are no monomer−monomer interactions. Our protein Hamiltonian choice is guided by our desire to study hydrophobic collapse in the absence of bias toward a compact oligomer state. In our model, hydrophobic collapse emerges naturally from an explicit treatment of hydrogen bond entropy.[26,30]

It is important to point out that the lattice model described above was formulated[30] on the assumption that the conformational equilibria of hydrophobic oligomers can be modeled using the small-solute description of hydrophobicity. This appears to be a sound assumption based on previous modeling efforts by some of us,[26] as well as theoretical considerations implying that the hydrophobic solvation of short n-alkanes (with 20 or fewer C atoms) can be described in terms of the small-solute solvation thermodynamics of its constituent monomers.[2] For longer chainlike hydrophobic solutes, the model will need to be reformulated in order to include many-body hydration effects.

3. SIMULATION METHOD

The lattice model was studied using the density of states (DOS) algorithm by Wang and Landau (WL).[28,29] We chose the WL method over the traditional Metropolis Monte Carlo (MC) given our interest in studying cold unfolding of hydrophobic oligomers. The MC technique generates configurations with a probability equal to an un-normalized Boltzmann distribution, $p(E_o \rightarrow E_n) = \exp(-(\Delta E)/k_B T)$, where k_B is Boltzmann's constant, T the absolute temperature, and ΔE the total potential energy difference between the original (E_o) and trial (E_n) configurations. At low temperatures or at first-order phase transitions,[42] $|\Delta E| \gg k_B T$, leading to low acceptance probabilities and, consequently, pervasive meta-

dx.doi.org/10.1021/jp3039237 | J. Phys. Chem. B 2012, 116, 9540−9548

stability. The WL algorithm circumvents this shortcoming by performing a random walk in energy, in which configurations are accepted with probability proportional to $1/\Omega(E)$, where $\Omega(E)$, the DOS, is computed on-the-fly (i.e., the DOS is constantly updated). Having computed $\Omega(E)$, one can in principle calculate the temperature dependence of any observable from a single simulation (see below). The WL algorithm can be summarized as follows.[28,29,43] Beginning with an initial configuration, the DOS is initialized to $\Omega(E) = 1$ for all discrete energy levels, E. Similarly, a histogram recording the number of visits per energy state is initialized to $H(E) = 0$. Within a predefined energy range, the random walk proceeds, attempting a series of moves (involving both the oligomer and water, see below), which are accepted with probability

$$p(E_o \rightarrow E_n) = \min\left[1, \frac{\Omega(E_o)}{\Omega(E_n)}\right] \tag{2}$$

where E is the potential energy of the protein-water system and o and n denote the starting and new configurations, respectively. In practice, the ratio of the density of states is computed as $\exp(\ln \Omega(E_o) - \ln \Omega(E_n))$. Every time an energy state is visited, its corresponding DOS is updated following $\Omega(E) \rightarrow \Omega(E)f$, where $f > 1$ is a modification factor initialized to $f = e \approx 2.718....$ Similarly, the energy histogram is updated as $H(E) \rightarrow H(E) + 1$. As a practical matter, one implements the DOS modification as $\ln \Omega(E) \rightarrow \ln \Omega(E) + \ln f$. The modifications of $\Omega(E)$ and $H(E)$ apply regardless of whether the configuration is the modified state after acceptance of the move or the old configuration after rejection. Density of states modification proceeds until all energy states have been visited a sufficient number of times, e.g., when $H(E) \geq H_{min}$ or $H(E)/\langle H\rangle \geq 0.8$ for all E.[44] In this work, we have chosen the former criterion, setting $H_{min} = 100$. We also ran a simulation with $H_{min} = 1000$, finding results in agreement with those of the more relaxed convergence criterion (see Supporting Information). Once one of the latter criteria is met, the energy histogram is considered flat and the modification factor is reduced according to the recursion $\ln f_{i+1} = 1/2 \ln f_i$. Also, the energy histogram is reinitialized to zero (but not the density of states) and the simulation proceeds, modifying the DOS with the updated modification factor. The simulation continues until a desired reduction of the modification factor is attained, at which point $\ln \Omega$ is known to an accuracy proportional to $\ln f$.

In all simulations discussed below, $q = 84$. This parameter value (determining the number of water orientations), together with the ground state energy (E_{min}, see below) resulted in convergence of our simulations within a time frame of CPU years. Although higher q values were not explored on practical grounds, we were able to capture similar oligomer structural features as in simulations[30] with $q = 168$. The flatness of $H(E)$ is checked every 1000 sweeps in which several moves (accepted with a probability given by eq 2) are attempted in a randomly chosen sequence. These include rotations and translations of water molecules.[52] A number of oligomer chain modifications were attempted every sweep, including the following:[23−25,30] (1) Reptation moves, in which a terminal monomer is clipped from one end of the oligomer chain and reattached at the other end. (2) Reorientation of two monomers at the chain end. (3) Three-bond kink motions in which a sequence of three bonds in a gauche± conformation is modified to its "conjugate", i.e., gauche± → gauche∓. (4) Four-bond kink motions in which a sequence of two consecutive gauche conformations with opposite sign is inverted, i.e., gauche± gauche∓ → gauche∓ gauche±. In all moves attempted, water molecules and monomers were randomly selected. For oligomer moves, the sites to which the move is attempted can be occupied by a water molecule (in which case the monomers and waters exchange positions) or unoccupied, but they may not be initially occupied by a monomer.

A salient aspect of the WL method is that it readily lends itself to computer parallelization.[30,43] This is particularly important for systems such as ours, where the broad energy range ($E_{min} \approx -2420$ kcal/mol at the lowest solvent density, and $E_{min} \approx -3250$ kcal/mol at the highest) and, consequently, long sampling times, would render the calculation prohibitive if it were run on a single processor. The WL algorithm allows the energy range to be subdivided in different subranges or "windows", each of which is run in a separate processor. The energy range of the systems discussed in this work was subdivided into 16 windows. Overlapping regions between windows have a size equal to half their width.[30] During the simulation, configurations in the overlapping region between two windows are used as the initial configuration in the lower energy window. If the low-energy configuration is trapped in a potential energy minimum, this swap provides an escape pathway.[30,43,45] Once the window simulations converge, the full density of states is obtained by shifting each window's DOS to obtain agreement at the overlapping regions.[43]

3.1. Data Analysis. We compute $\Omega(E)$ to within a modification factor accuracy of $\ln f \approx 1 \times 10^{-6}$. With the converged density of states, we perform a WL simulation with fixed transition rates. Every time an energy state is visited we record the values of a number of observables O, as well as the number of visits per state, $H(E)$. Once all energy states are visited at least 100 times, the random walk in energy is considered converged, providing the average value of the observable as a function of energy,

$$\overline{O(E)} = \frac{1}{H(E)} \sum_{x \in E}^{H(E)} O(x) \tag{3}$$

where x runs over configurations with energy E.[30,45] The temperature dependence of O can be subsequently computed by reweighting the observable in an appropriate ensemble. For our canonical ensemble (constant number of particles, temperature, and number of lattice sites),

$$\langle O(T)\rangle = \sum_E \overline{O(E)} p(E, T) \tag{4}$$

where $p(E,T)$ is the microstate probability in the canonical ensemble,

$$p(E, T) = \frac{\Omega(E)\exp(-\beta E)}{\sum_E \Omega(E)\exp(-\beta E)} \tag{5}$$

where $\beta = 1/k_B T$. We compute $\overline{O(E)}$ from at least 4 (typically, 12−15) independent simulations, each of which is initialized with different random configurations of the solvated oligomer, and a random number of generator seeds.

The applicable energy range over which the WL simulation is performed is dictated by the temperature range over which $\langle O(T)\rangle$ is to be computed. To ensure that all states contributing to a canonical ensemble are adequately sampled, we have verified that $p(E,T)$ (eq 5) gives rise to a distribution with a clear peak, with the maximum value of $p(E,T)$ much

dx.doi.org/10.1021/jp3039237 | J. Phys. Chem. B 2012, 116, 9540−9548

greater than the values of $p(E,T)$ at the low- and high-energy ends of the distribution.[46]

We study systems composed of a hydrophobic decamer solvated in N = 270, 291, 310, and 400 water molecules on a lattice of B = 432 sites in periodic boundary conditions, corresponding to fractional densities ($\rho_f = N/B$) of 0.63, 0.67, 0.72 and 0.93, respectively. The number of hydrogen bonds per molecule when ρ_f = 0.72, 3.46 ± 0.03 (determined from a canonical MC simulation at T^* = 0.13, T = 300 K), is close to the value determined from MD simulations of the SPC/E water model at 300 K and a mean density of 0.993 g cm^{-3}, 3.6 per molecule.[47] This suggests that oligomer collapse is investigated near physiological conditions of density.

We have analyzed oligomer conformations in terms of the radius of gyration, R_g, given by

$$R_g = \left(\frac{1}{2N_m^2} \sum_i \sum_j |\mathbf{r}_i - \mathbf{r}_j|^2 \right)^{1/2} \quad (6)$$

where $\mathbf{r}_i$ is the position vector of monomer i and N_m = 10 is the number of residues. Other quantities computed include the number of hydration water molecules (i.e., those adjacent to at least one monomer), N_{Hyd}, the number of trans and gauche rotational conformations (N_t, and N_g, respectively[54]), as well as the number of monomer−water−monomer contacts (water bridges, N_B). In the data presented next, the error was estimated using the jackknife binning method among the 4+ runs.[48]

In the following, we discuss the thermodynamics of a solvated hydrophobic oligomer, using the terms unfolding and denaturation interchangeably and rather liberally. Denaturation is intimately linked to the loss of biological activity, whose description demands much greater detail than is afforded by our coarse-grained protein. Consequently, a caveat is warranted as to the use of "denaturation", which, in this context, should be interpreted as the loss of a compact, relatively dry, oligomer conformation.

4. RESULTS AND DISCUSSION

Ensemble-average structural properties of the solvated oligomer and its hydration layer are presented in Figures 2 and 3. Data are reported as a function of the reduced temperature $T^* = k_B T/\varepsilon_{HB}$, where ε_{HB} = 4.54 kcal/mol is a typical HB energy. Figure 2a presents the temperature dependence of the radius of gyration (eq 6) of the hydrophobic oligomer at several solvent fractional densities. Up to ρ_f = 0.72, $\langle R_g \rangle$ is approximately parabolic in the neighborhood of T^* = 0.2, evidencing thermal unfolding characterized by extended oligomer configurations at $T^* > 0.3$ for all densities, and cold unfolding at $T^* < 0.1$. The oligomer is maximally compact at $T^* \approx 0.19$ for all densities. As previously observed by Matysiak et al.,[30] the cold denatured state is more compact than its thermally denatured counterpart. This is in agreement with experimental observations on apomyoglobin and β-lactoglobulin in 4 M urea,[8] which imply that the cold denatured state is a relatively compact structure, quite different from extended thermally denatured proteins. Contrary to its behavior at low and intermediate densities, we note that the $\langle R_g \rangle$ profile at ρ_f = 0.93 shows a slight monotonic increase with T^*. On the basis of $\langle R_g \rangle$, cold denaturation appears to be suppressed at ρ_f = 0.93. A similar observation was reported in a MD study of hydrophobic oligomer hydration with the Jagla model of water,[49,50] in which the cold-unfolding transition is shown to vanish at high pressure. Similarly, at ρ_f = 0.93, the behavior of $\langle R_g \rangle$ at high temperatures indicates only moderate thermal expansion, an observation that contrasts with the sudden increase in $\langle R_g \rangle$ at lower densities. It will subsequently be shown that at ρ_f = 0.93 the oligomer is denatured for all T^* (vide infra). It should be noted that low-temperature error bars tend to be larger throughout because of the inherently low degeneracy of the DOS of low energy configurations.

The number of hydration-layer water molecules ($\langle N_{Hyd} \rangle$) presented in Figure 2b also shows a parabolic dependence at

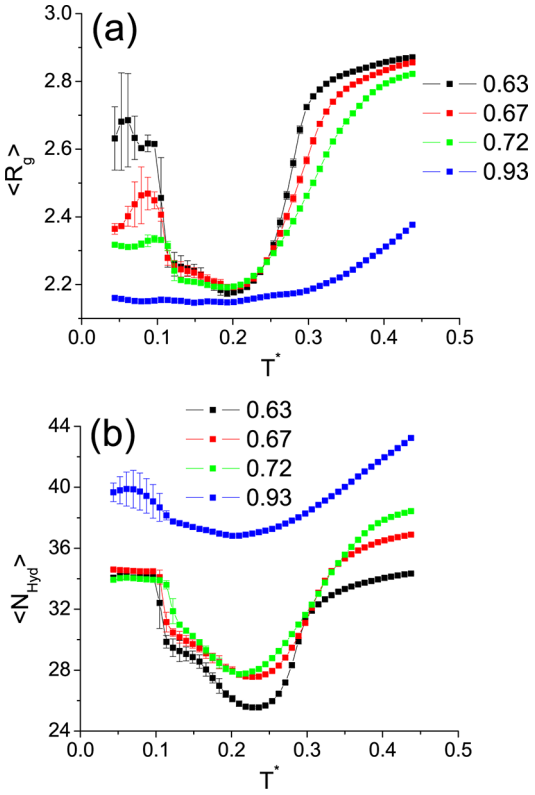

Figure 2. Temperature dependence of the radius of gyration ($\langle R_g \rangle$, a) and the number of hydration-layer water molecules ($\langle N_{Hyd} \rangle$, b) of a solvated decamer at various solvent fractional densities, indicated in the caption.

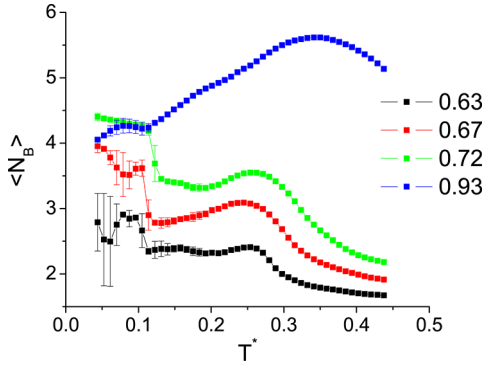

Figure 3. Temperature dependence of the number of monomer−water−monomer contacts ("water bridges", $\langle N_B \rangle$) of a solvated decamer at various solvent fractional densities, indicated in the caption. A molecule forms a water bridge if it is adjacent (nearest neighbor) to two residues that are, themselves, separated by three or more monomers along the chain sequence.

dx.doi.org/10.1021/jp3039237 | J. Phys. Chem. B 2012, 116, 9540−9548

intermediate temperature. As remarked by Davidovic et al.[8] and Matysiak et al.,[30] although they are relatively compact, cold-unfolded proteins have a water-penetrated hydrophobic core.[8] Therefore, the data in Figure 2b are in agreement with inference from NMR experiments:[8] more water molecules constitute the hydration layer at $T^* < 0.1$, a consequence of partial unfolding and residue solvent-exposure. At higher temperatures and densities in the range 0.63−0.72, there is a decrease of between six and nine water molecules in $\langle N_{Hyd} \rangle$ upon oligomer collapse from the cold-unfolded state, followed by an increase in $\langle N_{Hyd} \rangle$ as the oligomer is thermally denatured, exposing more monomers to the solvent. The minimum in $\langle N_{Hyd} \rangle$ for $\rho_f \leq 0.72$ is a manifestation of the hydrophobic effect: by minimizing the number of monomers exposed to the solvent, which impose an entropic penalty on hydration water, the entropy of the system is maximized. We note that at $\rho_f = 0.93$, the $\langle N_{Hyd} \rangle$ profile exhibits a parabolic dependence on T^*, at odds with the approximate monotonic increase in $\langle R_g \rangle$ at the same density (Figure 2a). The decrease in $\langle N_{Hyd} \rangle$ (~3 water molecules) upon heating from low to intermediate T^* is much smaller than that observed at lower solvent densities. While the minimum in $\langle N_{Hyd} \rangle$ at high ρ_f could be interpreted as a weak signature of hydrophobic collapse, the behavior of the radius of gyration suggests otherwise, because the oligomer is compact for all T^*. On the basis of the analysis of the oligomer hydrophobic core presented next, we will argue that high solvent density forces denaturation of the oligomer for all T^*.

To demonstrate this view, we have computed the number of monomer−water−monomer contacts (water bridges, $\langle N_B \rangle$). $\langle N_B \rangle$ is defined as the number of water molecules adjacent to two monomers placed a minimum of three residues apart on the oligomer chain (i.e., when a water molecule is nearest neighbor to monomers i and $j \geq i + 3$). This definition renders $\langle N_B \rangle$ a meaningful property to quantify the extent to which the core of a compact oligomer is water penetrated and, consequently, a good indicator for pressure- and cold-denaturation.[8,11] The temperature dependence of $\langle N_B \rangle$ is shown in Figure 3. We first discuss behavior for $\rho_f \leq 0.72$. Within this density range, the dependence of $\langle N_B \rangle$ on T^* can be interpreted as follows. $\langle N_B \rangle$ is maximal at low T^*, evidencing a strongly water-penetrated, but compact, hydrophobic core, characteristic of the cold-unfolded oligomer;[8] upon heating up to $T^* \approx 0.1$, $\langle N_B \rangle$ decreases by ~1, indicating the expulsion of a water molecule from the hydrophobic core upon folding. At $T^* > 0.2$, the onset of thermal denaturation first results in thermal expansion of the globule, which allows a slight increase in the number of waters that can be accommodated in the hydrophobic core (note the local maximum in $\langle N_B \rangle$ at $T^* \approx 0.25-0.26$); at higher temperatures ($T^* > 0.25$) the oligomer is thermally unfolded, the hydrophobic core breaks down, and a monotonic decrease in $\langle N_B \rangle$ is observed. Conversely, the system at high density ($\rho_f = 0.93$) does not show an intermediate T^* range where $\langle N_B \rangle$ is at a local minimum and, therefore, no indication of hydrophobic collapse. We note, instead, that the number of water bridges is high throughout, with the value of $\langle N_B \rangle$ being at least as high as that of the cold denatured oligomer at $\rho_f = 0.72$. Increasing the temperature results in thermal expansion of the globule and the number of water molecules that intrude into the hydrophobic core (note the increase in $\langle N_B \rangle$ up to $T^* \approx 0.34$), followed by breakdown of the hydrophobic core, signaled by the decrease in $\langle N_B \rangle$, at the highest T^*. This trend is consistent with the increase in $\langle R_g \rangle$ (cf., Figure 2a for $\rho_f = 0.93$). The data in Figures 2 and 3, therefore, lead us to conclude that the oligomer solvated at high density ($\rho_f = 0.93$) is denatured and can be described as an ensemble of compact, but strongly water-penetrated, oligomer configurations.

In addition to variations in the compactness and hydration layer structure, what are the distinguishing structural features of folded and unfolded oligomer conformations? To address this question, we have computed the number of trans and gauche rotational conformations ($\langle N_t \rangle$ and $\langle N_g \rangle$, respectively), whose T^* profile is shown in Figure 4. Both rotational conformations

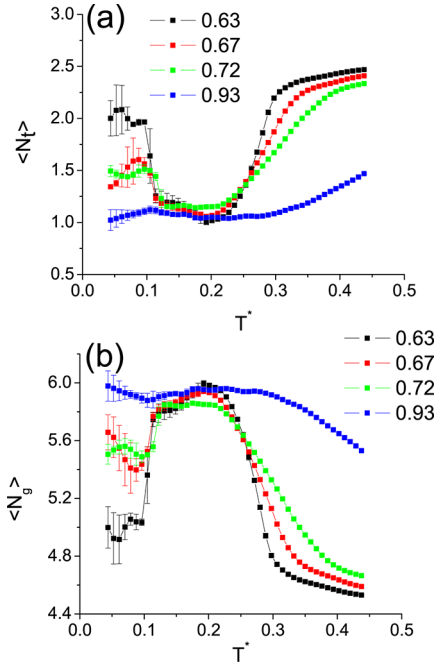

Figure 4. Temperature dependence of the number of trans ($\langle N_t \rangle$, a) and gauche states ($\langle N_g \rangle$, the sum of gauche+ and gauche−, b) of a solvated decamer at various solvent fractional densities, indicated in the inset.

exhibit a roughly parabolic dependence on temperature (inverted in the case of gauche states) for $\rho_f < 0.93$. Folded states significantly favor gauche states over trans: the maximally compact (folded) oligomer ($T^* \approx 0.19$) is composed of ~1 trans state vs ~6 gauche states. An increase of up to 1 trans state is observed in the cold denatured conformations prevalent at $T^* < 0.1$; as expected, the thermally unfolded oligomers also show an increase of ~1−2 trans states. At high density ($\rho_f = 0.93$), an oligomer conformation composed of ~1 trans and ~6 gauche states predominates up to $T^* \approx 0.3$; at higher T^*, thermal expansion leads to a slight increase in the number of trans states (see Figure 4a for $\rho_f = 0.93$). We note that $\langle N_g \rangle$ (Figure 4b) is equal to the sum of the gauche+ and gauche− rotational conformations; both gauche states are equally likely (the Hamiltonian is unbiased).

Figure 5 shows configurations of the hydrophobic oligomer (shown in gray, with gray lines representing monomer−monomer covalent bonds) obtained from the simulations with $\rho_f = 0.63$ (left panel, Figures 5a−c) and $\rho_f = 0.93$ (right panel, Figures 5d−f). Yellow spheres are water molecules involved in monomer−water−monomer contacts; yellow bonds joining water molecules, if any, represent HBs. In Figure 5 energy (temperature) increases from top to bottom. Configurations a and d of Figure 5 were obtained from the lowest energy

dx.doi.org/10.1021/jp3039237 | J. Phys. Chem. B 2012, 116, 9540−9548

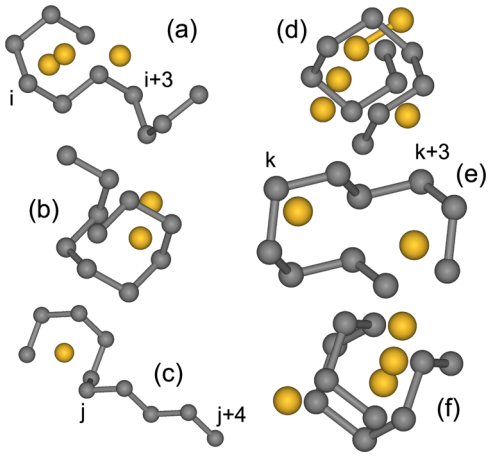

Figure 5. Renderings of representative configurations of the hydrophobic oligomer in the lattice. Gray spheres and lines denote monomers and monomer–monomer covalent bonds, respectively. Yellow spheres denote water molecules involved in monomer–water–monomer contacts (water bridges). Bonds between two waters (if any) denote HBs. Left panel: ρ_f = 0.63; right panel: ρ_f = 0.93. Configurations a and d were obtained from the lowest energy window, b and e are representative of systems at $T^* \approx 0.2$, and c and f were obtained from the highest energy window. Monomers labeled *i*, *j*, or *k* are involved in trans rotational states (see text).

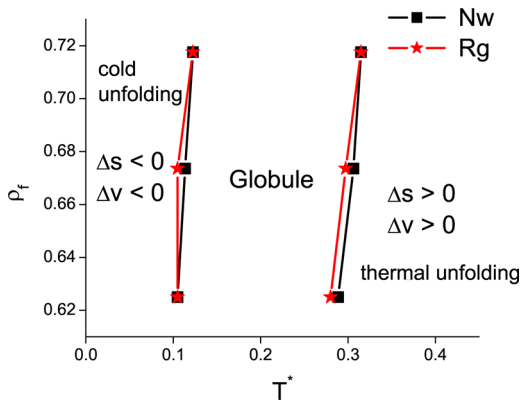

Figure 6. ρ_f–T^* "phase diagram" of a solvated hydrophobic oligomer. The cold and thermal unfolding temperatures were estimated from maxima in $d\langle R_g\rangle/dT^*$ and $d\langle N_{Hyd}\rangle/dT^*$ (see Figure 2 and Supporting Information).

window in the WL simulations, which encompasses cold-unfolded states. Configurations b and e of Figure 5were obtained from the energy window containing the most probable state of a canonical ensemble at $T^* = 0.2$ (determined from the Boltzmann distribution, not shown) while configurations c and f of Figure 5 were obtained from the highest energy window, within which thermally unfolded configurations are sampled. The oligomer conformations belonging to the low-density system show characteristics of the cold-unfolded, folded, and thermally unfolded states discussed above: Figure 5b, representative of the folded state, is compact, showing a suppression of trans states; upon cooling, it expands (note the appearance of a trans state between residues *i* and *i* + 3 in Figure 5a), and its hydrophobic core undergoes water penetration; upon heating (Figure 5c) the oligomer unfolds, increasing its trans character (note the two terminal trans states between residues *j* and *j* + 4). Conversely, oligomer configurations obtained from the system at ρ_f = 0.93 are compact and show significant water penetration. The compactness of the oligomers is reflected in a predominance of gauche states, although oligomers with trans states are also sampled, as evident, for example, in the trans conformation involving residues *k* to *k* + 3 shown in Figure 5e.

Using the structural information of Figure 2 we have constructed a "phase diagram" for the solvated hydrophobic oligomer. The cold- and thermal-unfolding temperatures were located at the point where $d\langle R_g\rangle/dT^*$ and $d\langle N_{Hyd}\rangle/dT^*$ show local extrema (see Supporting Information). The results are presented in Figure 6. We first note the good agreement between the conformational transition temperatures, as determined from numerical differentiation of $\langle R_g\rangle$ and $\langle N_{Hyd}\rangle$, all within 0.01. Furthermore, we observe that the transition loci are positively sloped within the range of density studied. This observation is in agreement with the typical observed phenomenology at low and intermediate pressures for proteins.[26,32] Further, we note that the 2-D model of Patel et al.[26] did not exhibit a positive slope of the thermal-unfolding curve because of a direct link between lattice volume and the number of HBs (which decreases upon unfolding) in the model formulation. The 3-D lattice model of Matysiak et al.,[30] upon which this work is based, can manifest this typical slope of the thermal unfolding curve because the total volume of the system is not directly linked to the number of HBs.[55] The slope of the coexistence curves provides information about entropy and volume changes upon unfolding, a link that is established by the Clausius–Clapeyron equation. Cold-unfolding is characterized by $\Delta s < 0$ and $\Delta v < 0$, where *s* and *v* are the molar entropy and volume of the system (solvent and oligomer). It is generally accepted that the entropy of the system decreases mainly from the exposure of hydrophobic monomers to water, and there is a decrease in the molar volume from the better packing of water molecules as they penetrate the hydrophobic core of the oligomer.[11] On the other hand, molar entropy and volume increase upon thermal unfolding at low (ambient) pressure because of the thermal expansion of the solvent and the extended conformations that the unfolded chain adopts at high T^*.[56] Finally, we should note that, in experiments, the melting (thermal-unfolding) curve becomes negatively sloped at high pressures[26,32] and that, with increasing *p*/density, the cold and thermal-unfolding curves meet at a common temperature, resulting in a characteristic dome-shaped phase diagram.[32,50] In our work, we were unable to close the phase diagram because of the progressive broadening of the thermal denaturation transition at densities higher than ρ_f = 0.72. Nonetheless, our data at ρ_f = 0.93, a condition under which the oligomer is denatured for all T^*, provides indirect evidence that the phase diagram would, indeed, close at an intermediate density between 0.72 and 0.93.

5. SUMMARY AND CONCLUSIONS

We have presented a simulation study of a three-dimensional lattice model of a hydrophobic oligomer in explicit water, focusing on the effect of solvent density and temperature on the stability of the oligomer. We find that at solvent fractional densities on the lattice between 0.63 and 0.72, the oligomer exhibits cold- and thermally induced unfolding transitions. The former gives rise to a still compact but strongly water-penetrated oligomer conformation, while the latter is characterized by unfolding to structures resembling a random coil. The folded state possesses a largely dry hydrophobic core and a compact geometry where gauche rotational conforma-

dx.doi.org/10.1021/jp3039237 | J. Phys. Chem. B 2012, 116, 9540–9548

tions predominate. Results of a simulation at high solvent density (ρ_f = 0.93) suggest that the oligomer is pressure-denatured, its conformation being compact and water-penetrated for all T^*. The phase diagram presented in Figure 6 shows that the model captures the typical positive slope of both the cold- and thermal-unfolding curves with increasing pressure, at low and intermediate density. Progressive weakening of the conformational transition signatures at higher density precludes us from determining whether the model implemented would capture the correct sign of the high-pressure branch of the melting curve, although high density results suggest that it must.

Possible avenues for future work include a closer examination of the folded state, particularly the presence of solvent-excluded void volumes in the hydrophobic core, which, alongside folded state energetics, are thought to determine native state volumetric properties.[57] While the energetic contribution to the folded volume cannot be accounted for by our coarse-grained protein representation, it should be possible to examine the temperature dependence of the number of void lattice sites within the folded hydrophobic core. To this end, longer oligomers than considered here will have to be used to effectively shield the hydrophobic core from the solvent. A further direction for future inquiry involves a closer examination of the conformational transitions undergone by the solvated oligomer. The broad thermal unfolding transition reported in this work suggests a second-order-like transition, whereas the more sudden increase of the radius of gyration at low T^* suggests first-order-like behavior for cold-unfolding. Investigation of conformational equilibria at low densities (i.e., where water is under tension) would also be worth pursuing. In addition, the three-dimensional nature of the model enables the study of protein secondary structure, through the addition of monomer−monomer interactions. Future work along these lines will focus on the analysis of T^*-stability of helical oligomers.

■ ASSOCIATED CONTENT

Supporting Information

Details of the calculation of conformational transition loci, solvent phase behavior, verification of convergence, and lattice model parametrization. This material is available free of charge via the Internet at http://pubs.acs.org.

■ AUTHOR INFORMATION

Corresponding Author

*E-mail: santiago.romero-vargas@yale.edu.

Present Address

[⊥]Department of Chemical and Environmental Engineering, Yale University, New Haven, CT 06520.

Notes

The authors declare no competing financial interest.

■ ACKNOWLEDGMENTS

P.G.D. and P.J.R. gratefully acknowledge the financial support of the National Science Foundation (Collaborative Research in Chemistry Grants CHE-0908265 (P.G.D.) and CHE-0404695 (P.J.R.)), and the R.A. Welch Foundation (grant F0019 to P.J.R.). S.R.-V.C. acknowledges useful discussions with Sumit Sharma and Sapna Sarupria. The simulations presented in this article were performed on computational resources supported by the Princeton Institute for Computational Science and Engineering (PICSciE) and the Office of Information Technology's High Performance Computing Center and Visualization Laboratory at Princeton University.

■ REFERENCES

(1) Kauzmann, W. *Adv. Protein Chem.* **1959**, *14*, 1−63.
(2) Chandler, D. *Nature* **2005**, *437* (7059), 640−647.
(3) Dill, K. A. *Biochemistry* **1990**, *29* (31), 7133−7155.
(4) Southall, N. T.; Dill, K. A.; Haymet, A. D. J. *J. Phys. Chem. B* **2002**, *106* (3), 521−533.
(5) Frank, H. S.; Evans, M. W. *J. Chem. Phys.* **1945**, *13* (11), 507−532.
(6) Rossky, P. J.; Zichi, D. A. *Faraday Symp. Chem. Soc.* **1982**, *17*, 69−78.
(7) Zichi, D. A.; Rossky, P. J. *J. Chem. Phys.* **1985**, *83* (2), 797−808.
(8) Davidovic, M.; Mattea, C.; Qvist, J.; Halle, B. *J. Am. Chem. Soc.* **2009**, *131* (3), 1025−1036.
(9) Pangali, C.; Rao, M.; Berne, B. J. *J. Chem. Phys.* **1979**, *71* (7), 2982−2990.
(10) Kauzmann, W. *Nature* **1987**, *325* (6107), 763−764.
(11) Hummer, G.; Garde, S.; Garcia, A. E.; Paulaitis, M. E.; Pratt, L. R. *Proc. Natl. Acad. Sci. U.S.A.* **1998**, *95* (4), 1552−1555.
(12) Hummer, G.; Garde, S.; Garcia, A. E.; Paulaitis, M. E.; Pratt, L. R. *J. Phys. Chem. B* **1998**, *102* (51), 10469−10482.
(13) Cheung, M. S.; Garcia, A. E.; Onuchic, J. N. *Proc. Natl. Acad. Sci. U.S.A.* **2002**, *99* (2), 685−690.
(14) Zhou, R. H.; Huang, X. H.; Margulis, C. J.; Berne, B. J. *Science* **2004**, *305* (5690), 1605−1609.
(15) Zhou, R. H.; Berne, B. J.; Germain, R. *Proc. Natl. Acad. Sci. U.S.A.* **2001**, *98* (26), 14931−14936.
(16) Zhou, R.; Germain, R.; Berne, B. J. *Abstracts of Papers*, 223rd National Meeting of the American Chemical Society, Orlando, FL, Apr 7−11, 2002; American Chemical Society: Washington, DC, 2002; U505
(17) Garcia, A. E.; Sanbonmatsu, K. Y. *Proteins Struct., Funct. Genet.* **2001**, *42* (3), 345−354.
(18) Garcia, A. E.; Onuchic, J. N. *Proc. Natl. Acad. Sci. U.S.A.* **2003**, *100* (24), 13898−13903.
(19) Sarupria, S.; Garde, S. *Phys. Rev. Lett.* **2009**, *103* (3), 037803.
(20) Lau, K. F.; Dill, K. A. *Macromolecules* **1989**, *22* (10), 3986−3997.
(21) De Los Rios, P.; Caldarelli, G. *Phys. Rev. E* **2000**, *62* (6), 8449−8452.
(22) Marques, M. I.; Borreguero, J. M.; Stanley, H. E.; Dokholyan, N. V. *Phys. Rev. Lett.* **2003**, *91* (13), 138103.
(23) Kolinski, A.; Skolnick, J.; Yaris, R. *Biopolymers* **1987**, *26* (6), 937−962.
(24) Skolnick, J.; Kolinski, A.; Yaris, R. *Biopolymers* **1989**, *28* (6), 1059−1095.
(25) Sikorski, A.; Skolnick, J. *Biopolymers* **1989**, *28* (6), 1097−1113.
(26) Patel, B. A.; Debenedetti, P. G.; Stillinger, F. H.; Rossky, P. J. *Biophys. J.* **2007**, *93* (12), 4116−4127.
(27) Patel, B. A.; Debenedetti, P. G.; Stillinger, F. H.; Rossky, P. J. *J. Chem. Phys.* **2008**, *128* (17), 175102.
(28) Wang, F. G.; Landau, D. P. *Phys. Rev. Lett.* **2001**, *86* (10), 2050−2053.
(29) Wang, F. G.; Landau, D. P. *Phys. Rev. E* **2001**, *64* (5), 056101.
(30) Matysiak, S.; Debenedetti, P. G.; Rossky, P. J. *J. Phys. Chem. B* **2012**, DOI: 10.1021/jp3039175.
(31) Athawale, M. V.; Goel, G.; Ghosh, T.; Truskett, T. M.; Garde, S. *Proc. Natl. Acad. Sci. U.S.A.* **2007**, *104* (3), 733−738.
(32) Hawley, S. A. *Biochemistry* **1971**, *10* (13), 2436−2442.
(33) Roberts, C. J.; Debenedetti, P. G. *J. Chem. Phys.* **1996**, *105* (2), 658−672.
(34) Roberts, C. J.; Panagiotopoulos, A. Z.; Debenedetti, P. G. *Phys. Rev. Lett.* **1996**, *77* (21), 4386−4389.
(35) Truskett, T. M.; Debenedetti, P. G.; Sastry, S.; Torquato, S. *J. Chem. Phys.* **1999**, *111* (6), 2647−2656.

(36) Poole, P. H.; Sciortino, F.; Grande, T.; Stanley, H. E.; Angell, C. A. *Phys. Rev. Lett.* **1994**, *73* (12), 1632−1635.
(37) Matysiak, S.; Debenedetti, P. G.; Rossky, P. J. *J. Phys. Chem. B* **2011**, *115* (49), 14859−14865.
(38) Rezus, Y. L. A.; Bakker, H. J. *Phys. Rev. Lett.* **2007**, *99* (14), 148301.
(39) Bowron, D. T.; Filipponi, A.; Roberts, M. A.; Finney, J. L. *Phys. Rev. Lett.* **1998**, *81* (19), 4164−4167.
(40) Laage, D.; Stirnemann, G.; Hynes, J. T. *J. Phys. Chem. B* **2009**, *113* (8), 2428−2435.
(41) Richardson, J. S., Richardson, D. C. Prediction of Protein Structure and the Principles of Protein Conformation. In *Principles and Patterns of Protein Conformation*; Plenum: New York, 1989.
(42) Challa, M. S. S.; Landau, D. P.; Binder, K. *Phys. Rev. B* **1986**, *34* (3), 1841−1852.
(43) Shell, M. S., Panagiotopoulos, A. Z., Pohorille, A. Methods Based on Probability Distributions and Histograms. In *Free Energy Calculations. Theory and Applications in Chemistry and Biology*; Springer: New York, 2007.
(44) Shell, M. S.; Debenedetti, P. G.; Panagiotopoulos, A. Z. *Phys. Rev. E* **2002**, *66* (5), 056703.
(45) Rampf, F.; Binder, K.; Paul, W. *J. Polym. Sci., Part B: Polym. Phys.* **2006**, *44* (18), 2542−2555.
(46) Parsons, D. F.; Williams, D. R. M. *Phys. Rev. E* **2006**, *74* (4), 041804.
(47) Kumar, R.; Schmidt, J. R.; Skinner, J. L. *J. Chem. Phys.* **2007**, *126* (20), 204107.
(48) Weigel, M.; Janke, W. *Phys. Rev. E* **2010**, *81* (6), 066701.
(49) Buldyrev, S. V.; Kumar, P.; Debenedetti, P. G.; Rossky, P. J.; Stanley, H. E. *Proc. Natl. Acad. Sci. U.S.A.* **2007**, *104* (51), 20177−20182.
(50) Buldyrev, S. V.; Kumar, P.; Sastry, S.; Stanley, H. E.; Weiner, S. *J. Phys.: Condens. Matter* **2010**, *22* (28), 284109.
(51) Canchi, D. R.; Paschek, D.; Garcia, A. E. *J. Am. Chem. Soc.* **2010**, *132* (7), 2338−2344.
(52) At low temperature, the lattice model of water used in our work may crystallize to an open, ordered phase similar to cubic ice, or a close-pack, ordered structure analogous to ice VII.[33] In order to study the properties of the oligomer without confounding effects due to solvent freezing, we reject all moves leading to nucleation of either of the aforementioned crystal phases.
(53) We note that in the original model by Roberts and Debenedetti[33] only HB interactions are weakened by nearest neighbors.
(54) A rotational state is defined for every three bonds (equivalently, every 4 monomers). Hence, a 10-residue oligomer has a maximum of 7 rotational conformations.
(55) We note that protein denaturation is typically analyzed in the $p-T$ plane,[26,32] whereas we provide a $\rho-T$ phase diagram. We note, however, that slopes of coexistence lines in the $p-T$ and $\rho-T$ planes have the same sign because $dp/dT = (dp/d\rho)\,(d\rho/dT)$ and, for a stable thermodynamic system, $dp/d\rho > 0$. Hence, the positive slope determined in the $\rho-T$ plane translates into a positive slope in the $p-T$ plane.
(56) Our simulations were conducted on a rigid lattice. Nonetheless, it is possible to conceptualize volume changes at the cold- and thermal-unfolding transitions by considering a smaller control subvolume, whose dimensions fluctuate, that encompasses the solvated oligomer. When the oligomer cold-unfolds, hydrophobic core penetration causes the number of water molecules within the control subvolume, N_{sv}, to increase (see Figure 3); this is equivalent to reducing the size of the control subvolume at constant N_{sv}. Similarly, at the thermal unfolding transition, thermal expansion of the solvent will result in an increase of the control subvolume at fixed N_{sv}.
(57) Royer, C.; Winter, R. *Curr. Opin. Colloid Interface Sci.* **2011**, *16* (6), 568−571.